ARTICLE

OBC
www.rsc.org/obc

Directed, selective insertion of single molecules into patterned self-assembled monolayers of alkanethiols with different chain lengths

Xue-Mei Li, Tommaso Auletta, Frank C. J. M. van Veggel,† Jurriaan Huskens * and David N. Reinhoudt *

Laboratory of Supramolecular Chemistry and Technology, MESA$^+$ Institute for Nanotechnology, University of Twente, P.O. Box 217, 7500 AE Enschede, The Netherlands

Received 9th October 2003, Accepted 24th November 2003
First published as an Advance Article on the web 15th December 2003

Pd(II) pincer adsorbate molecules (**1**) were inserted into self-assembled monolayers (SAMs) of alkanethiols with different chain lengths (C_8 to C_{18}) on annealed gold substrates. Their presence was brought to expression by reaction of **1** with Au nanoclusters bearing phosphine moieties (**2**). The surface-confined Au nanoclusters were observed only on the shorter chain SAMs (C_8SH to C_{16}SH) and not on C_{18}SH SAMs. This is attributed to the longer chain length of C_{18}SH preventing the insertion of pincer molecules. Microcontact printing (μCP) with C_{18}SH on unannealed gold substrates and the subsequent immersion of the substrates into C_8SH, C_{10}SH, C_{12}SH, or C_{16}SH solutions, yielded a series of patterned SAMs that have areas of thiols of different chain lengths. Insertion of **1** followed by expression using **2**, or insertion of **3** showed inserted molecules only in the shorter chain SAM areas. The absolute particle densities in the former case were higher than on the corresponding homogeneous SAMs on annealed substrates, probably due to larger numbers of defects in the SAMs on unannealed substrates.

Introduction

Self-assembled monolayers (SAMs) are highly ordered monomolecular thin films formed spontaneously by chemisorption and self-organization of long chain molecules on the surface of appropriate substrates.[1] Self-assembled monolayers have found many applications such as in nanofabrication,[2–5] nanoelectronics,[6–13] biological screening,[14] and analytical chemistry.[15,16] Patterned SAMs have been fabricated by microcontact printing (μCP).[17,18] These have been applied as resists for pattern transfer[19] and as templates for patterning proteins and other biosystems.[14,20] SAMs with nanosized domains have been patterned by dip-pen nanolithography (DPN),[4,21–23] nanografting,[24] and constructive lithography[25,26] resulting in high lateral resolution. The thinnest patterns reported to date are of a few tens of nanometers with DPN.[22b]

A relatively easy bottom-up method to obtain individual isolated molecules is the slow exchange of thiols of SAMs with a solution of another ligand that has a sulfur moiety.[27] Based on this principle, single isolated molecules were obtained by the insertion of pyridine pincer molecules modified with a dialkyl sulfide moiety (**1**) into preformed SAMs.[28,29] Subsequently, a phosphine group present on monolayer-protected gold nanoclusters (MPCs) was attached to these pincer molecules by substitution of the pyridine ligand. Individual MPCs were visualized by scanning probe microscopy (SPM). This approach has provided a methodology to insert and detect single molecules embedded in a SAM. However, there is no control over the position and distribution of the single molecules.

So far, patterning of individual molecules or particles has been described in few reports.[30] To achieve this, combinations of top-down and bottom-up approaches may result in such methodologies.[31] μCP[17,18] is one of the most often used top-down approaches to create patterns of desired functional units.

In this paper we describe the selective insertion of pincer molecules (**1**) into surfaces patterned with alkanethiols that have different chain lengths as prepared by microcontact printing. The inserted molecules were visualized by using phosphine-functionalized MPCs. We address the insertion yield as a function of adsorbate chain length and gold substrate type (annealed or evaporated).

Results and discussion

The preparation of pincer molecule **1**, phosphine-functionalized MPCs **2**, and dendritic wedge **3** (Chart 1) has been reported elsewhere.[29,32] Both the pincer molecule **1** and the dendritic wedge **3** have a thioether moiety, which enables the anchoring to gold. Phosphine-functionalized MPCs **2** were prepared by reduction of Au(III) ions in the presence of decanethiol and 11-mercapto-1-undecanol, followed by esterification of the hydroxyl groups with 4-(biphenyl)phosphinobenzoic acid. The core size was 2.0 ± 0.5 nm as determined by transmission electron microscopy (TEM).[29]

Insertion of pincer molecules into SAMs of thiols with different chain lengths

Homogeneous self-assembled monolayers (SAMs) of alkanethiols on Au(111) were prepared by immersion of freshly H_2 flame-annealed gold-coated glass slides (used for easy visualization by AFM) into alkanethiol solutions. The alkanethiols employed were octanethiol (C_8SH), decanethiol (C_{10}SH), undecanethiol (C_{11}SH), dodecanethiol (C_{12}SH), hexadecanethiol (C_{16}SH), and octadecanethiol (C_{18}SH). These SAMs were immersed into a solution of **1**. Subsequently, the substrates were treated with a solution of **2**. The substrates were rinsed and imaged by tapping mode AFM in air. As shown in Fig. 1, the images reveal the presence of nanosize objects with a height of 3.5 ± 0.4 nm on the SAMs of C_8SH, C_{10}SH, C_{11}SH, C_{12}SH, and C_{16}SH. The height of the features matches very well the size of the nanoparticles including the ligand shell and it is comparable to previously reported results.[29] The appearance of **2** on the surface is therefore used as a probe for the insertion of **1** (Fig. 1). On the C_{18}SH SAM, no such objects were observed.

The number of particles we counted in the atomically flat areas of the annealed substrates was 20 ± 8 particles per μm^2 for

† *Present address*: University of Victoria, Department of Chemistry, P.O. Box 3065, Victoria, BC Canada V8W 3V6

DOI: 10.1039/b312422c

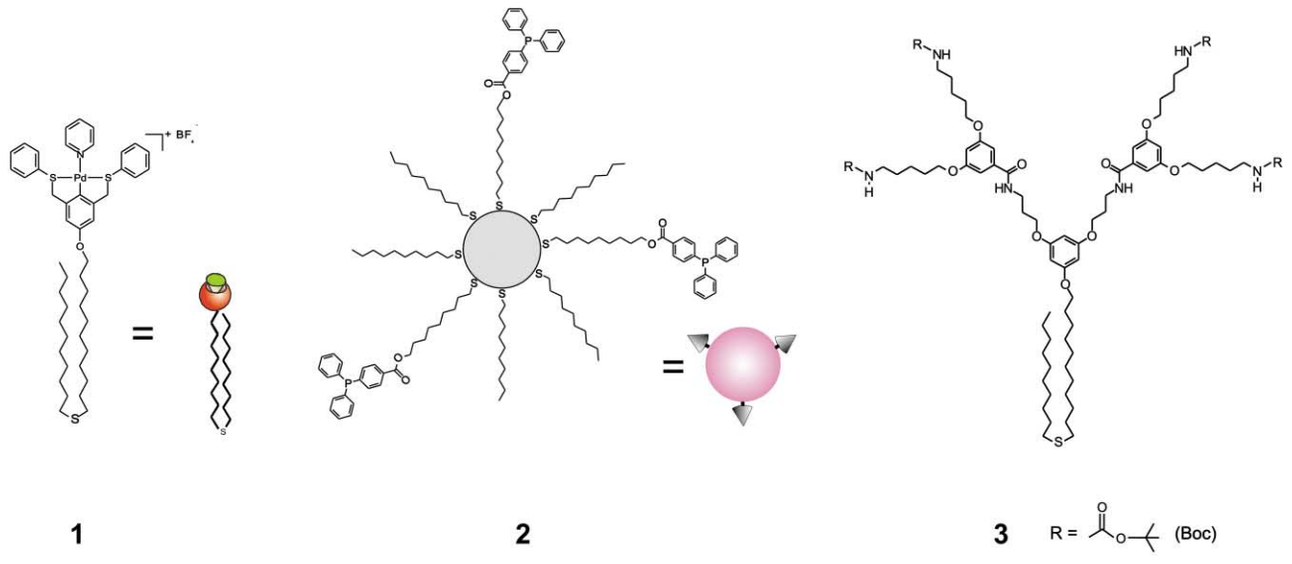

Chart 1

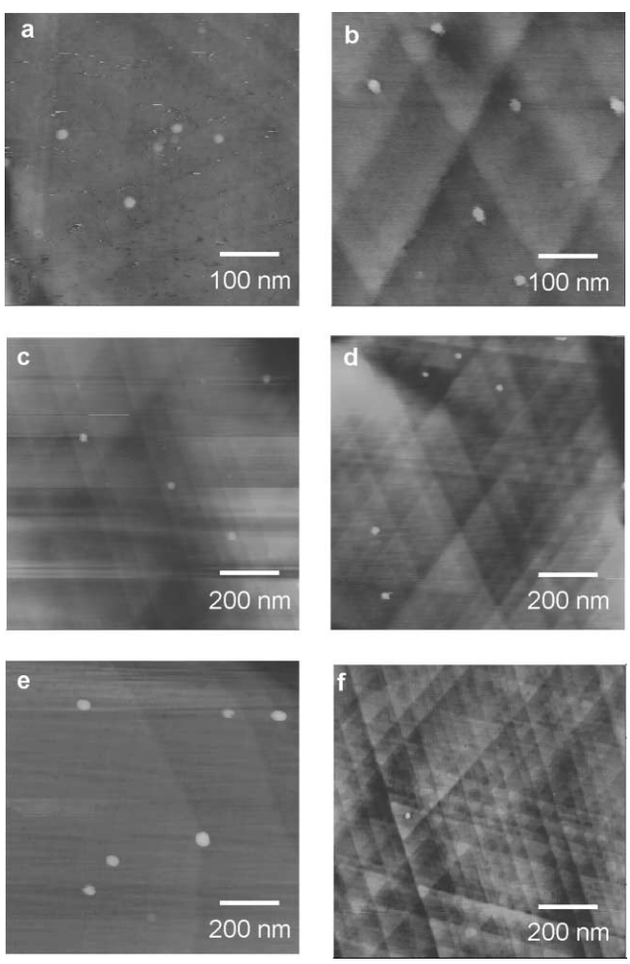

Fig. 1 Tapping mode AFM height images (z range 10 nm) of C_8SH (a), $C_{10}SH$ (b), $C_{11}SH$ (c), $C_{12}SH$ (d), $C_{16}SH$ (e), and $C_{18}SH$ (f) SAMs after insertion of pincer **1** and subsequent immobilization of **2**.

C_8SH and $C_{10}SH$ SAMs, in good agreement with previous studies.[29,32] On $C_{11}SH$, $C_{12}SH$, and $C_{16}SH$ SAMs, AFM images showed 5 ± 2 particles per μm². This particle number difference on the shorter chain SAM (C_8, C_{10}) and longer chain (C_{11}–C_{16}) SAMs reflects that shorter chain SAMs are less well-ordered and tend to desorb more easily and thus show more insertion than the longer chain SAMs.[33] No odd/even chain length effect appeared to exist as witnessed by the presence of approximately equal amounts of particles on the $C_{11}SH$ and $C_{12}SH$ SAMs.

The absence of particles on the C_{18} SAMs may be attributed to three factors: (i) higher resistance of $C_{18}SH$ against desorption, (ii) inhibition of pincer insertion by steric requirements of the headgroup, (iii) embedding of the inserted pincer molecules in the SAM preventing the subsequent particle attachment. The desorption of thiols upon immersion in a solvent is related to the stability of the SAMs and thus, to the chain length of the adsorbate. When exposed to a solvent, longer chain alkanethiol SAMs are more stable owing to stronger interchain van der Waals interactions.[33] Since no distinct difference between $C_{16}SH$ and $C_{18}SH$ SAMs has been described in the literature, it is anticipated that ligand desorption has taken place on both SAMs. According to CPK models, the length of $C_{16}SH$ is 2.7 ± 0.1 nm, and of $C_{18}SH$ 3.0 ± 0.1 nm. The length of **1** from the sulfide atom to the Pd(II) center (2.7 ± 0.1 nm) is shorter than $C_{18}SH$. Since the pincer headgroup is large relative to the alkyl chain, it likely prevents insertion of the adsorbate. This is confirmed by results obtained with dendritic wedge **3** (see below).

Selective insertion of single molecules into patterned SAMs

Since no insertion was observed on the C_{18} SAMs, a selective insertion of the single molecules was conducted using patterned SAMs created by μCP. μCP relies on the conformal contact between the stamp and the substrate and ink transfer from the stamp to the substrate. As flame annealing leads to larger roughness on the μm scale, microcontact printing was performed on unannealed, evaporated, granular substrates for ease of visualization of the μm patterns. μCP was carried out by using $C_{18}SH$ as the ink and subsequent immersion of the microcontact printed substrates into one of the following thiol solutions: C_8SH, $C_{10}SH$, $C_{11}SH$, $C_{12}SH$, and $C_{16}SH$. The resulting patterned substrates are referred to as C_{18}/C_8, C_{18}/C_{10}, C_{18}/C_{11}, C_{18}/C_{12}, and C_{18}/C_{16} respectively. These substrates were imaged by tapping mode AFM. Fig. 2 shows images of C_{18}/C_{12} and C_{18}/C_{16} substrates.[34] The broader stripes in the images are the $C_{18}SH$ areas. The height differences are attributed to the chain length differences and the phase differences to tip-surface interactions. For C_{18}/C_8, C_{18}/C_{10}, C_{18}/C_{11}, and C_{18}/C_{12} substrates, the AFM images showed that different thiol areas are discernible both in height and phase images. For the C_{18}/C_{16} substrate, the contrast in height is not clearly observable, but a phase contrast is still clearly visible.

These substrates were subjected to the same insertion process of **1** followed by attachment of **2** as described above for the homogeneous SAMs and as is shown in Scheme 1. To locate the MPCs, scanning of a relatively large area was first carried out, which provides information on the locations of different thiol

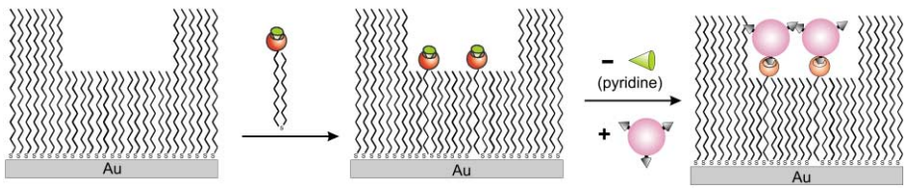

Scheme 1

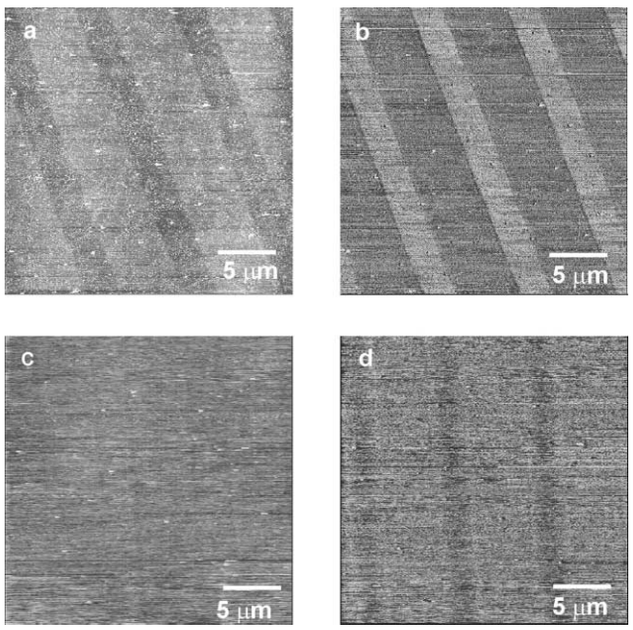

Fig. 2 Tapping mode AFM height (a, c) (z range 10 nm) and phase (b, d) (z range 20°) images of microcontact printed substrates: C_{18}/C_{12} (a, b) and C_{18}/C_{16} (c, d), prepared by printing of $C_{18}SH$ and subsequent immersion in a solution of a second thiol.

areas. Then these areas were imaged separately by zooming in on 1 × 1 μm² or smaller areas for visualizing the nanoparticles.

Fig. 3 shows height and phase images of different areas of a C_{18}/C_8 substrate. The gold surface morphology is granular at this scale. The presence of MPCs was determined by combination of the height and phase images. Figs 3a and 3b show the height and phase images of a C_8 area of a C_{18}/C_8 substrate. The nanoparticles appeared as smaller "grains" in the height profile, but showed a different phase profile.[35] Very few MPCs were observed in the $C_{18}SH$ areas of these micropatterned substrates (Figs 3c and d).[36] The same selective insertion was also observed on other micropatterned substrates: C_{18}/C_{16}, C_{18}/C_{12}, C_{18}/C_{11}, C_{18}/C_{10}.

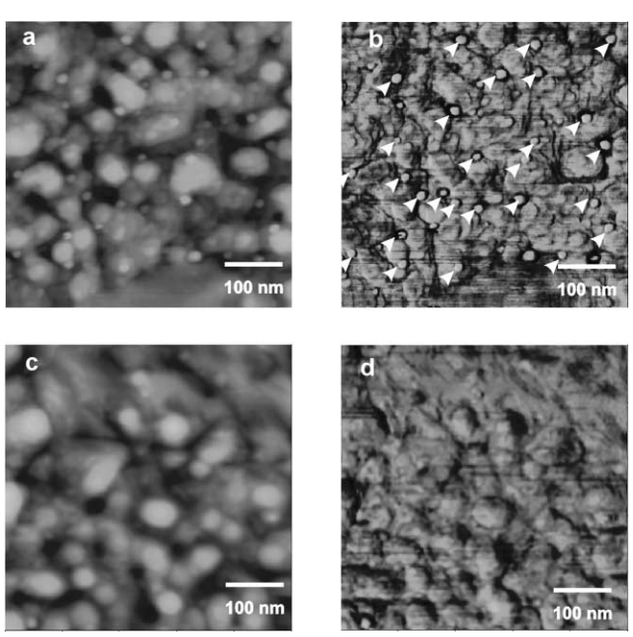

Fig. 3 AFM height (a, c) (z range 10 nm) and phase (b, d) (z range 20°) images of the C_8 (a,b) and C_{18} (c,d) areas of a microcontact printed C_{18}/C_8 substrate after pincer **1** insertion and gold nanoparticle **2** immobilization. White markers indicate the gold nanoparticles in image b.

The numbers of particles in the C_8SH areas of the C_{18}/C_8 substrates were much higher than on C_8SH SAMs on annealed gold substrates, which may be ascribed to less well-ordered SAMs on the granular substrates used in μCP leading to enhanced insertion. The same trend was also found for the C_{18}/C_{10} C_{18}/C_{11}, C_{18}/C_{12}, and C_{18}/C_{16} substrates. For comparison, the numbers of particles per μm² are plotted both for annealed (used for homogeneous SAMs) and unannealed (used for μCP) substrates (Fig. 4). For SAMs of C_8SH–$C_{12}SH$, more particles were found on unannealed substrates, while for $C_{16}SH$, the numbers of particles were in the same range as for annealed substrates.

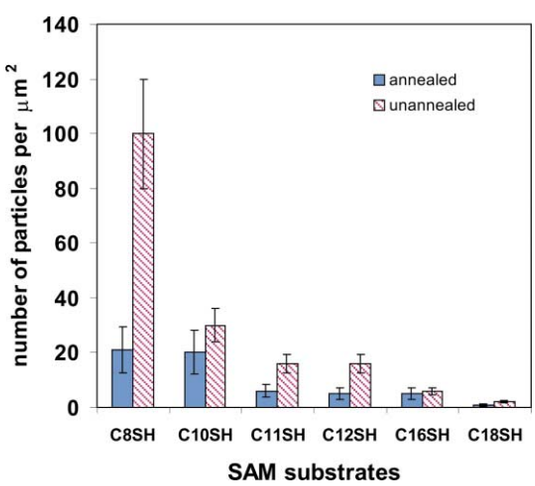

Fig. 4 Numbers of immobilized gold nanoparticles per μm² on SAMs of different thiols on annealed and unannealed substrates, as observed by AFM after insertion of **1** followed by immobilization of **2**.

The same directed insertion strategy was applied to direct the immobilization of the dendritic wedge **3** (Chart 1) on a gold surface. Wedge **3** possesses a thioether moiety, which provides the anchoring point for immobilization on gold. Furthermore, the dendritic wedges have large headgroups, which can more easily be detected by SPM without the need of expression. Gold substrates with prepatterned areas were created by microcontact printing of $C_{18}SH$ on gold, followed by wet etching. The etching step allows an immediate and easy recognition of the contacted and noncontacted areas, although it is not absolutely needed as shown above. The grooves in between the printed areas were then filled by immersing the substrates in a $C_{10}SH$ solution (1 mM in ethanol) for 2 h. The patterned surface was imaged by TM-AFM and the two thiol areas were easily discriminated in the height image (Fig. 5).

Subsequently, the substrate was immersed in a solution of **3** (0.01 mM) for 2 h. After careful rinsing, the substrate was imaged by TM-AFM. TM-AFM images in air showed the presence of nanosize features with an average height of 7.0 ± 1.5 nm, exclusively in the $C_{10}SH$ areas (Fig. 6a). The height

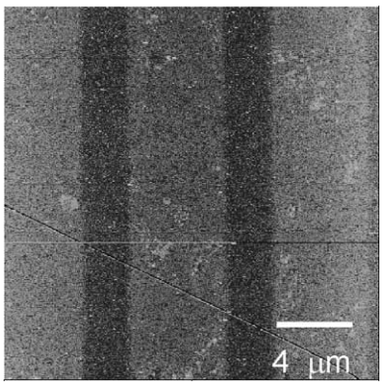

Fig. 5 A TM-AFM height image (z range 20 nm) of a C_{18}/C_{10} micropatterned substrate prepared by μCP of $C_{18}SH$, followed by wet etching and subsequent immersion into a $C_{10}SH$ solution.

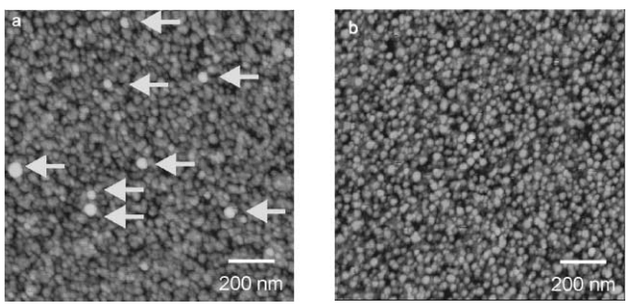

Fig. 6 TM-AFM height images (z range 10 nm) of the $C_{10}SH$ (a) and $C_{18}SH$ (b) areas after exposure to a 0.01 mM solution of dendrimer wedge **3** in CH_2Cl_2 for 2 h.

profile of the $C_{18}SH$ areas did not show any nanosize feature corresponding to single isolated dendritic structures (Fig.6b).[37] Because here the insertion process itself is imaged, the absence of single molecules in the $C_{18}SH$ areas can be directly attributed to the inhibition of the insertion of adsorbate **3**, most likely because of steric hindrance. The height values measured for the inserted molecules were in the same order of magnitude as previously reported.[32,38] No systematic evaluation of the width of the dendrimers has been carried out, due to the tip convolution issue.[39] The average number of nanometer-sized features counted in the $C_{10}SH$ area was 20 ± 8 per μm^2, in good agreement with the pincer insertion (see above).[29]

Conclusions

Self-assembled monolayers of alkanethiols with different chain lengths (C_8SH, $C_{10}SH$, $C_{11}SH$, $C_{12}SH$, $C_{16}SH$, $C_{18}SH$) on gold have been used as the matrix SAMs to study the insertion of pincer molecule **1**. Phosphine-functionalized MPCs **2** were used as a probe to detect the presence of pincer molecules in the SAMs. AFM showed that pincer molecule **1** was inserted into C_8SH, $C_{10}SH$, $C_{11}SH$, $C_{12}SH$, and $C_{16}SH$ SAMs but not in $C_{18}SH$ SAMs, which was ascribed to the chain length of the latter inhibiting the insertion of the adsorbate. This was confirmed by the insertion results of dendritic wedge **3**. This selectivity difference allowed the selective insertion of the adsorbate molecules **1** and **3** into areas of shorter thiols present at patterned SAMs prepared by μCP of $C_{18}SH$. This process combines microcontact printing, a top-down process, and self-assembly by insertion, a bottom-up approach, which we view as an important paradigm for nanofabrication.

Experimental

Chemicals

All chemicals were used as received, unless otherwise stated. Octanethiol (C_8SH), decanethiol ($C_{10}SH$), undecanethiol ($C_{11}SH$), dodecanethiol ($C_{12}SH$), hexadecanethiol ($C_{16}SH$), and octadecanethiol ($C_{18}SH$) were purchased from Aldrich. High purity water was obtained by Millipore membrane filtration. The preparation of pincer molecule **1**,[29] phosphine-functionalized MPCs **2**,[29] and dendritic wedge **3** has been described elsewhere.[32]

Substrate preparation

All glassware used for monolayer preparation was immersed in piranha solution (concentrated H_2SO_4 and 33% aqueous H_2O_2 in a 3 : 1 ratio). **CAUTION**: Piranha solution should be handled with care it has been reported to detonate unexpectedly. The glassware was rinsed with a large amount of water (Millipore).

Monolayer preparation

For homogeneous SAMs, gold substrates were obtained from Metallhandel Schröer GmbH (Lienen, Germany). Immediately before use, the substrates were rinsed with high-purity water (Millipore) and then flame-annealed with a H_2 flame (purity 6). Afterwards, the substrates were placed in pro analysi (p.a.) ethanol for 10 min and immersed into a freshly prepared adsorbate solution for 3 h at room temperature. The substrates were taken out and rinsed with copious amounts of methylene chloride, ethanol, and water.

Microcontact printing (μCP)

PDMS stamps were prepared according to a published procedure.[40] Gold substrates (Metallhandel Schröer GmbH) were treated with piranha for 1 min, and then rinsed with copious amounts of water and blown dry. A PDMS stamp was inked with 1 mM octadecanethiol in ethanol and was then blown dry under a stream of N_2. This procedure was repeated two or three times. The stamp was brought into contact with the freshly cleaned and dried gold substrate for 10–20 s. After releasing the stamp, the substrate was immersed in a 1 mM solution of a second thiol (C_8SH, $C_{10}SH$, $C_{11}SH$, $C_{12}SH$, or $C_{16}SH$) in ethanol for 3 h. Alternatively, after the printing step, the substrates were thoroughly washed with ethanol and then subjected to a ferro/ferricyanide etchant.[41] The etchant was prepared immediately before use by mixing an aqueous solution of $Na_2S_2O_3$ (0.1 M) and an aqueous solution containing KOH (1 M), $K_3Fe(CN)_6$ (0.01 M), and $K_4Fe(CN)_6$ (0.001 M) in a 1 : 1 ratio. After washing with high purity water (Millipore), the substrates were immersed in a 0.01 mM solution of $C_{10}SH$ in ethanol for 2 h. The samples were then removed from the solution, and rinsed thoroughly with dichloromethane, ethanol, and water (Millipore).

Insertion of adsorbates and nanoparticle immobilization

Solutions of **1** were deoxygenated prior to immersion of the monolayers by bubbling N_2 through the solutions for 10 min. Homogeneous SAMs or microcontact printed SAMs were immersed in the solutions of **1** for 3 h. After rinsing, the substrates were immersed in the phosphine-functionalized gold nanoparticle **2** solution for 10 min. The samples were rinsed by placing them in CH_2Cl_2 (20 mL) three times, each time for 5 min. For the insertion of adsorbate **3**, a patterned substrate (C_{18}/C_{10}) prepared by microcontact printing and wet etching was immersed in a 0.01 mM solution of adsorbate **3** for 2 h and then rinsed by placing it in CH_2Cl_2.

Atomic force microscopy (AFM)

The AFM measurements were carried out using a NanoScope III multimode AFM (Digital Instruments, Santa Barbara, CA, USA). Tapping mode AFM scans were performed in air using silicon cantilevers/tips (Nanosensors, Wetzlar, Germany; cantilever resonance frequency f_0 = 280–320 kHz). The free

amplitude was kept constant for all experiments and the amplitude damping (set point) ratio was adjusted to ≈0.90. Prior to the measurements, the setup was thermally equilibrated for several hours in order to minimize the drift and to ensure a constant temperature (≈30 °C). The piezo scanner was calibrated in the lateral directions using a grid with repeat distances of 1.0 μm, as well as self-assembled monolayers of thiols on Au(111) (*e.g.* octadecanethiol, repeat distance 0.51 nm), and in the z-direction by measuring step heights of Au(111) (2.9 Å). The number of nanometer-size features and their standard deviations were determined by counting the features on at least three areas of the same sample, and taking the average.

Acknowledgements

This research is supported by the Technology Foundation STW, applied science division of NWO and the technology program of the Ministry of Economic Affairs (XML: project number: TST4946) and the Council for Chemical Sciences of the Netherlands Organization for Scientific Research (CW-NWO) (TA: grant number 97041). The authors are grateful to Dr. Henk-Jan van Manen for the kind donation of adsorbates **1** and **3**.

References and Notes

1 A. Ulman, *An Introduction to Ultrathin Organic Films*, Academic Press, Boston, 1991.
2 N. A. Amro, S. Xu and G. Y. Liu, *Langmuir*, 2000, **16**, 3006–3009.
3 R. Maoz, E. Frydman, S. R. Cohen and J. Sagiv, *Adv. Mater.*, 2000, **12**, 424–429.
4 S. H. Hang and C. A. Mirkin, *Science*, 2000, **288**, 1808–1811.
5 X. M. Zhao, Y. N. Xia and G. M. Whitesides, *J. Mater. Chem*, 1997, **7**, 1069–1074.
6 C. Joachim, J. Gimzewski and A. Aviram, *Nature*, 2001, **408**, 541–548.
7 P. S. Peercy, *Nature*, 2000, **406**, 1023–1026.
8 J. Chen, M. A. Reed, A. M. Rawlett and J. M. Tour, *Science*, 1999, **286**, 1550–1552.
9 D. I. Gittins, D. Bethell, D. J. Schiffrin and R. J. Nichols, *Nature*, 2000, **408**, 67–79.
10 C. P. Collier, G. Mattersteig, E. W. Wong, Y. Luo, K. Beverly, J. Sampaio, F. M. Raymo, J. F. Stoddart and J. R. Heath, *Science*, 2000, **289**, 1172–1175.
11 Z. D. Cui, A. Primak, X. Zarate, J. Tomfohr, O. F. Sankey, A. L. Moore, D. Gudt, G. Harris and S. M. Lindsay, *Science*, 2001, **294**, 571–574.
12 J. M. Tour, *Acc. Chem. Res.*, 2000, **33**, 791–804.
13 T. Vondrak, H. Wang, P. Winget, C. J. Cramer and X. Y. Zhu, *J. Am. Chem. Soc.*, 2000, **122**, 4700–4707.
14 R. S. Kane, S. Takayama, E. Ostuni, D. E. Ingber and G. M. Whitesides, *Biomaterials*, 1999, **20**, 2363–2376.
15 B. A. Grzybowski, R. Haag, N. Bowden and G. M. Whitesides, *Anal. Chem.*, 1998, **70**, 4645–4652.
16 H. Andersson, C. Jonsson, C. Moberg and G. Stemme, *Talanta*, 2002, **56**, 301–308.
17 Y. N. Xia and G. M. Whitesides, *Angew. Chem., Int. Ed.*, 1998, **37**, 551–575.
18 B. Michel, A. Bernard, A. Bietsch, E. Delamarche, M. Geissler, D. Juncker, H. Kind, J.-P. Renault, H. Rothuizen, H. Schmid, P. Schmidt-Winkel, R. Stutz and H. Wolf, *IBM J. Res. Dev.*, 2001, **45**, 697–719.
19 Y. N. Xia, X. M. Zhao and G. M. Whitesides, *Microelectron. Eng.*, 1996, **32**, 255–268.
20 S. Zhang, L. Yan, M. Altman, M. Lassle, H. Nugent, F. Frankel, D. A. Lauffenburger, G. M. Whitesides and A. Rich, *Biomaterials*, 1999, **20**, 1213–1220.
21 R. D. Piner, J. Zhu, F. Xu, S. Hong and C. A. Mirkin, *Science*, 1999, **283**, 661–663.
22 (*a*) L. M. Demers, D. S. Ginger, S. J. Park, Z. Li, S. W. Chung and C. A. Mirkin, *Science*, 2002, **296**, 1836–1838; (*b*) H. Zhang, S. W. Chung and C. A. Mirkin, *Nano Lett.*, 2003, **3**, 43–45.
23 K. B. Lee, S. J. Park, C. A. Mirkin, J. C. Smith and M. Mrksich, *Science*, 2002, **295**, 1702–1705.
24 G.-Y. Liu, S. Xu and Y. Qian, *Acc. Chem. Res.*, 2000, **33**, 457–466.
25 R. Maoz, E. Frydma, S. R. Cohen and J. Sagiv, *Adv. Mater.*, 2000, **12**, 725–731.
26 R. Maoz, S. R. Cohen and J. Sagiv, *Adv. Mater.*, 1999, **9**, 55–61.
27 C. M. Wijmans and E. Dickinson, *Langmuir*, 1999, **15**, 8344–8348.
28 A. Friggeri, H. Schönherr, H.-J. van Manen, B.-H. Huisman, G. J. Vancso, J. Huskens, F. C. J. M. van Veggel and D. N. Reinhoudt, *Langmuir*, 2000, **16**, 7757–7763.
29 A. Friggeri, H.-J. van Manen, T. Auletta, X.-M. Li, S. Zapotoczny, H. Schönherr, G. J. Vancso, J. Huskens, F. C. J. M. van Veggel and D. N. Reinhoudt, *J. Am. Chem. Soc.*, 2001, **123**, 6388–6395.
30 V. Paraschiv, S. Zapotoczny, M. R. de Jong, G. J. Vancso, J. Huskens and D. N. Reinhoudt, *Adv. Mater.*, 2002, **14**, 722–726.
31 R. Glass, M. Arnold, J. Blümmel, A. Küller, M. Möller and J. P. Spatz, *Adv. Funct. Mater.*, 2003, **13**, 569–575.
32 H.-J. van Manen, T. Auletta, B. Dordi, H. Schönherr, G. J. Vancso, F. C. J. M. van Veggel and D. N. Reinhoudt, *Adv. Funct. Mater.*, 2002, **12**, 811–818.
33 M. D. Porter, T. B. Bright, D. L. Allara and C. E. D. Chidsey, *J. Am. Chem. Soc.*, 1987, **109**, 3559–3568.
34 The phase difference AFM images depend on the operating conditions, for example, different setpoint and amplitude setpoint can result in different phase contrast.
35 Due to tip convolution, the width of the nanoparticles appeared in the range of 20 to 30 nm instead of the real size.
36 The few particles may result from some exchange of $C_{18}SH$ for shorter thiols during the immersion step directly after μCP, allowing the insertion of **1** and immobilization of **2** in the subsequent steps.
37 As reference experiments, to exclude any interference of physisorbed material, patterned substrates were submitted to TM-AFM imaging (not shown here) prior to the exposure to the dendrimer **3** solution. No nanosized structures could be observed in either area, except the granular texture of the substrates themselves.
38 The granularity of unannealed substrates does not allow the setting of a unique zero level as reference for section analysis. As a consequence both the average and standard deviation of the height values measured for **3** after insertion are higher than reported for similar structures prepared on annealed substrates.
39 H. Schönherr, Ph. D. Thesis, University of Twente, The Netherlands, 1999.
40 X.-M. Zhao, Y. Xia and G. M. Whitesides, *J. Mater. Chem.*, 1997, **7**, 1069–1074.
41 Y. Xia, X. Zhao, E. Kim and G. M. Whitesides, *Chem. Mater.*, 1995, **7**, 2332–2337.